# Ionicity, Atomic Radii, and Structure in the Layered Dichalcogenides of Group IVb, Vb, and VIb Transition Metals

F. R. GAMBLE

*Corporate Research Laboratories, Esso Research and Engineering Company, Linden, New Jersey 07036*

Pauling's electronegativities are introduced in considerations of bond lengths, lattice constants, atomic radii, charge densities, structures, and heats of formation of the layered dichalcogenides of Groups IVb, Vb, and VIb transition metals. Strong correlations are found between these and the fractional ionic character of the metal–chalcogen bonds as defined by Pauling. A critical effective radius ratio is defined that separates trigonal prismatic and octahedral compounds.

## Introduction

A group of materials whose physical and chemical properties have stimulated considerable interest is the layered dichalcogenides of group IVb, Vb, and VIb transition metals (*1*), crystalline materials built from layers comprising a sheet of metal atoms sandwiched between two sheets of chalcogens. Within a layer, the bonds are strong, while between adjacent layers, they are remarkably weak, conferring on the crystals facile basic cleavage, lubricity, and marked anisotropy in many physical properties.

It is traditional and helpful to consider the crystal structures of these layered dichalcogenides in terms of close-packed layers of large spherical anions with small metal cations in certain of the interstices. The symmetry of the chalcogen array about each metal atom is either octahedral or trigonal prismatic (Fig. 1). Three of the trigonal prismatic compounds, $TaS_2$, $TaSe_2$, and $MoTe_2$, can be prepared with octahedral coordination or nearly octahedral coordination if they are quenched from high temperature or grown in the presence of excess chalcogen. The remaining compounds are known at room temperature only in the coordination indicated in Table I. The tellurides of Nb, Ta, and W crystallize in distorted versions of the octahedral structures where metal–metal bonding may play a role. The high-temperature phase of $MoTe_2$, metastable at room temperature, also has this kind of structure.

A number of workers have called attention to differences between the compounds that imply
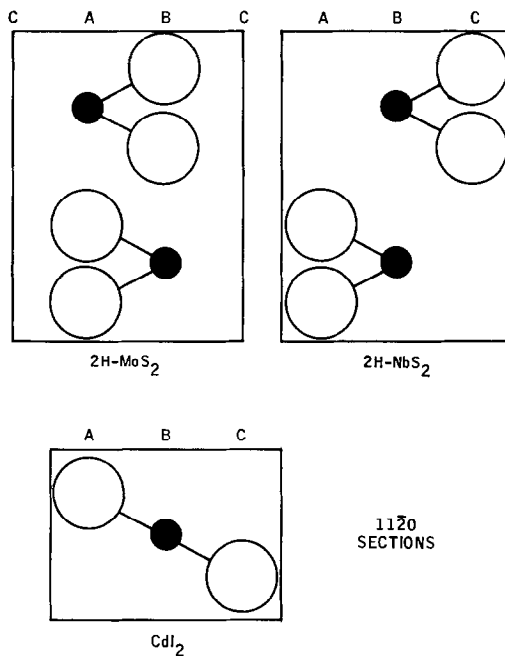


FIG. 1. The $11\bar{2}0$ sections of the three structures under consideration. In the 2H-$MoS_2$ structure (adopted by Group VIb dichalcogenides) and in the 2H-$NbS_2$ structure (Group Vb dichalcogenides), the chalcogens on each side of the layer superimpose. The metal atom is then in a site of trigonal prismatic symmetry. In those compounds adopting the 1T structure ($CdI_2$), the chalcogens are not superposed but are staggered. The resulting site symmetry is ideally octahedral or, if distorted, trigonal antiprismatic. In these structures it is possible for the chalcogens to approach the metal atom more closely before touching along the c-axis.

358

TABLE I

| | $\Delta X$ | $f_i$ | S | $a$ (Å) | $c$ (Å) | $d(MX)^a$ (Å) | Ref. |
|---|---|---|---|---|---|---|---|
| 1. $HfS_2$ | 1.2 | 0.30 | O | 3.635 | 5.837 | 2.56 | 1 |
| 2. $ZrS_2$ | 1.1 | 0.26 | O | 3.662 | 5.813 | 2.56 | 1 |
| 3. $HfSe_2$ | 1.1 | 0.26 | O | 3.748 | 6.159 | 2.66 | 1 |
| 4. $TiS_2$ | 1.0 | 0.22 | O | 3.405 | 5.690 | 2.42 | 1 |
| 5. $ZrSe_2^b$ | 1.0 | 0.22 | O | 3.770 | 6.138 | 2.66 | 1 |
| 6. $2H\text{-}NbS_2$ | 0.9 | 0.19 | T | 3.31 | $2 \times 5.945$ | 2.47 | 10 |
| 7. $2H\text{-}TaS_2$ | 0.9 | 0.19 | T | 3.315 | $2 \times 6.05$ | 2.48 | 1 |
| $1T\text{-}TaS_2$ | 0.9 | 0.19 | O | 3.36 | 5.90 | 2.44 | 11 |
| 8. $TiSe_2$ | 0.9 | 0.19 | O | 3.535 | 6.004 | 2.54 | 1 |
| 9. $VS_2^b$ | 0.8 | 0.15 | O | 3.29 | 5.66 | 2.37 | 10 |
| 10. $2H\text{-}WS_2$ | 0.8 | 0.15 | T | 3.154 | $2 \times 6.181$ | 2.41 | 1 |
| 11. $2H\text{-}NbSe_2$ | 0.8 | 0.15 | T | 3.442 | $2 \times 6.27$ | 2.595 | 12, 13 |
| 12. $2H\text{-}TaSe_2$ | 0.8 | 0.15 | T | 3.437 | $2 \times 6.362$ | 2.59 | 12 |
| $1T\text{-}TaSe_2$ | 0.8 | 0.15 | O | 3.477 | 6.272 | 2.55 | 1 |
| 13. $HfTe_2^b$ | 0.8 | 0.15 | O | 3.949 | 6.651 | 2.82 | 14 |
| 14. $2H\text{-}MoS_2$ | 0.7 | 0.12 | T | 3.160 | $2 \times 6.147$ | 2.42 | 1 |
| 15. $VSe_2^b$ | 0.7 | 0.12 | O | 3.352 | 6.104 | 2.47 | 1 |
| 16. $2H\text{-}WSe_2$ | 0.7 | 0.12 | T | 3.286 | $2 \times 6.488$ | 2.51 | 1 |
| 17. $ZrTe_2^b$ | 0.7 | 0.12 | O | 3.950 | 6.630 | 2.82 | 1 |
| 18. $2H\text{-}MoSe_2$ | 0.6 | 0.09 | T | 3.288 | $2 \times 6.460$ | 2.49 | 1 |
| 19. $TiTe_2$ | 0.6 | 0.09 | O | 3.766 | 6.491 | 2.717 | 1 |
| 20. $NbTe_2$ | 0.5 | 0.06 | "O" | | | | |
| 21. $TaTe_2$ | 0.5 | 0.06 | "O" | | | | |
| 22. $VTe_2$ | 0.4 | 0.04 | O | 3.6 | 6.45 | 2.67 | 1 |
| 23. $WTe_2$ | 0.4 | 0.04 | "O" | | | | |
| 24. $2H\text{-}MoTe_2$ | 0.3 | 0.02 | T | 3.517 | $2 \times 6.983$ | 2.73 | 1 |

[a] In only a few cases are accurate bond distances available from refined crystal structures. The $z$ parameter obtained for the chalgogens ($z$ chalcogen–$z$ metal) in the trigonal prismatic compounds varied in these cases from 0.130 to 0.132. Where refinements were not available we used 0.131. (Note that the ideal $z$ for 2H trigonal prismatic compounds is 0.137, not 1/8 as is often seen.) For octahedral coordination, the ideal $z$ value, 1/4, was used.

[b] Metal rich.

substantial differences in ionicity. Thus, optical studies (2–4) indicate an order of magnitude greater effective dynamic charge in the sulfides and selenides of Hf and Zr than in the corresponding compounds of Mo and W. In photoemission studies of $MoS_2$ and $NbSe_2$, McMenamin and Spicer (5) find that $MoS_2$ appears less ionic than $NbSe_2$. White and Lucovsky (4) have pointed out the coincidence between the ionic diameters of the chalcogens and the $a$-axis of the Hf and Zr compounds. Finally, Huisman et al. (6) have suggested that in $d^0$, $d^1$, and $d^2$ compounds, d-covalency provides a stabilizing factor for trigonal prismatic coordination (observed in the group VIb and some group Vb compounds) vs the more symmetric, electrostatically favored, octahedral coordination (seen in

the IVb and some Vb compounds and in one VIb compound).

To account for the charge distributions and chalcogen–chalcogen distances in some of these compounds, unconventional valence bond structures (chalcogen–chalcogen bonds, interlayer bonds) have recently been invoked (4). It has been suggested that the occurrence of metallic conductivity in certain of the compounds requires their separate treatment in consideration of bond distances and structure (4). Finally, a "structure dependence" of the effective charge has been suggested (4). We will show here that the variation in crystal parameters observed in the set of compounds considered can be viewed as a natural and remarkably smooth function of the elemental

electronegativity differences of the bonding atoms. In particular, it will be shown: that the distribution of charge in these compounds, the ionicity, is, to first order, determined by the elemental electronegativities and not by the structure as has been suggested (4); that the shorter intralayer and interlayer chalcogen–chalcogen distances in the group VIb dichalcogenides does not imply chalcogen–chalcogen bonds; rather it is the consequence of the smaller size of almost neutral chalcogens; and finally that the concept of metallic bonding in the metallic members of this class is unnecessary in consideration of the structure or lattice parameters of any of these compounds.

Finally, we shall show that the radii of the atoms in this series of compounds cannot be assigned from any set of ionic or covalent radii but will vary as a function of the electronegativity difference of the bonding atoms. Only after taking this variation into account can one determine which crystal structures are geometrically allowed. In this manner, we see that, while all the compounds can adopt octahedral coordination, only certain of the compounds *can* adopt trigonal prismatic coordination and these do so.

## The Pauling Electronegativity Scale

Pauling (7) suggested that the energy of a bond between two atoms, A and B, could be expressed as the arithmetic mean of the A–A and B–B bond energies plus a contribution that depends on the electronegativity difference between A and B. He proposed the following expression:

$$D(A-B) = \tfrac{1}{2}[D(A-A) + D(B-B)] + 23\,(X_A - X_B)^2,$$

where $D(A-B)$ is the A–B bond energy in kcal/mole, $D(A-A)$ and $D(B-B)$ are the corresponding homopolar bond energies, and $X_A$ and $X_B$ are the respective elemental electronegativities. The standard heat of formation, $Q$, of a binary compound of A and B is then given by the equation

$$Q = 23 \sum (X_A - X_B)^2,$$

where the indicated summation is over all bonds in the compound. (If the standard states of the elements involve multiple bonds, as in $O_2$ or $N_2$, additional terms are required.) Aside from an arbitrary additive constant, the $X_i$ are then obtained from the appropriate thermochemical data. The elemental electronegativities Pauling derived in this manner are given in Ref. 7. In what follows, it should be kept in mind that thermochemical data for the chalcogenides were not included as they were not available. In a recent consideration of the heats of formation of the compounds in the NbN family RY (R = Ti, Zr, Hf, V, Nb, or Ta, and Y = C, N,

TABLE II

| Element | $X^a$ | Shannon and Prewitt radii[b] | | | | | Pauling radii −2 | Slater radii | Effective metal radii | | |
|---|---|---|---|---|---|---|---|---|---|---|---|
| | | +6 | +5 | +4 | +3 | +2 | | | $R_S$ | $R_{SE}$ | $R_{TE}$ |
| Hf | 1.3 | | | 0.71 | | | | 1.55 | 0.74 | 0.79 | 0.85 |
| Zr | 1.4 | | | 0.72 | | | | 1.55 | 0.73 | 0.78 | 0.85 |
| Ti | 1.5 | | | 0.605 | 0.67 | 0.86 | | 1.40 | 0.72 | 0.77 | 0.83 |
| Ta | 1.6 | | 0.64 | 0.66 | 0.67 | | | 1.45 | (2H) 0.82 | 0.87 | — |
| | | | | | | | | | (1T) 0.76 | 0.81 | — |
| V | 1.7 | | 0.54 | 0.59 | 0.64 | 0.79 | | 1.35 | 0.73 | 0.79 | 0.87 |
| Nb | 1.6 | | 0.64 | 0.69 | 0.70 | 0.71 | | 1.45 | 0.82 | 0.87 | — |
| W | 1.7 | 0.60 | | 0.65 | | | | 1.35 | 0.83 | 0.87 | — |
| Mo | 1.8 | 0.60 | 0.63 | 0.65 | 0.67 | | | 1.45 | 0.84 | 0.85 | 0.97 |
| Te | 2.1 | | | | | | 2.21 | 1.40 | | | |
| Se | 2.4 | | | | | | 1.98 | 1.15 | | | |
| S | 2.5 | | | | | | 1.84 | 1.00 | | | |

*a* Pauling electronegativity.
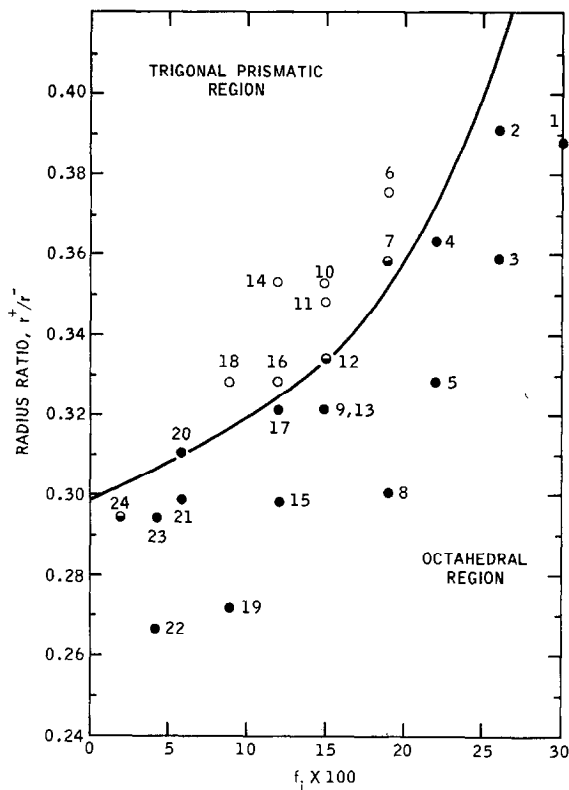*b* For six-fold coordination.

FIG. 2. The radius ratio $r^+/r^-$ versus the fractional ionic character $f_i$ of the metal–chalcogen bond. The ratio is computed using the Shannon and Prewitt ionic radii for cations of 4+ oxidation state and six-fold coordination (Table II). The anion radii are Pauling's ionic radii for the chalcogens in the 2– oxidation state. Open circles represent compounds in which the cation coordination is trigonal prismatic; solid circles, octahedral. The half solid circles represent compounds in which both configurations can be obtained at room temperature. The compounds can be identified by reference to Table I.

or O), Phillips (8) derived elemental electro-negativities that differ slightly from Pauling's. We elected to use the average of these two sets. These electronegativities are given in Table II. They differ from Pauling's only in the case of Ta and V, each of which are 0.1 greater than the Pauling values.

Pauling introduced the expression

$$f_i(A-B) = 1 - \exp{[-\tfrac{1}{4}(X_A - X_B)^2]},$$

where $f_i(A-B)$ is the fractional ionic character of the A–B bond (7). On expanding the exponential, one sees that for small electronegativity differences the "fractional ionic character" should be proportional to the heat of formation, $Q$. Below we shall show that this holds for the available data.

## Trigonal Prismatic vs Octahedral Coordination

If, as is suggested in Ref. 6, covalency favors trigonal prismatic coordination, one might conceivably order the compounds according to the difference in the electronegativities of the bonding elements and obtain a division of the two structures at some critical electronegativity difference. Such is not the case as can be seen by referring to Table I where the compounds are ordered according to this difference. However, a striking separation is possible if one plots the compounds on a radius ratio, $r^+/r^-$, vs ionicity diagram as shown in Fig. 2. An effective separation of trigonal prismatic from octahedral coordination can be made by drawing a gently curving line diagonally across the field. The ambivalent $TaS_2$, $TaSe_2$, and $MoTe_2$ are either

on or quite near the line. In this plot, the metal ionic radii used were those of Shannon and Prewitt for 4+ oxidation state and six-fold coordination (9). Because this set does not contain radii for $S^{2-}$, $Se^{2-}$, and $Te^{2-}$, we used Pauling's radii for these. In fact, however, the set of radii used in this plot is not critical. The Slater *atomic* radii (10) are substantially different from the *ionic* radii of Shannon and Prewitt and, yet, yield a similar, though not quite as effective, separation. Both sets of radii are given in Table II.

We were prompted to prepare the radius-ratio ionicity plots by the notion that the trigonal prismatic configuration with the chalcogens right above one another would be more likely if the radius-ratio, $r^+/r^-$, were large. This follows from the reasonable assumption that the bond distances in the chalcogenides of the metals under discussion are dictated by the elements bonding and not by the structure or the stoichiometry. For example, the Ti–S bond distances in all the titanium sulfides are nearly the same. The structure must permit the achievement of a "natural" metal chalcogen bond length. If we consider the bond length to be the sum of atomic radii, then the possible structures are determined by the radius ratio $r^+/r^-$. In the trigonal prismatic structure, the chalcogen atoms come into contact along the $c$-axis at a larger radius ratio (0.527) than in the octahedral structure (0.412). For ratios greater than 0.527 either structure is possible.

## The Effective Atomic Radii

At this point three questions arise: Why have we achieved the separation of structures using ionic radii when the compounds are mainly covalent? What are the effective radii that should obtain in these compounds? How can we understand the position and slope of the line separating the two structures?

One preliminary test of any set of radii is of course to see if they sum to give the correct bond distances. Here we must keep in mind that the bond distances in most of the compounds under consideration are known only approximately, the typical uncertainty running about 0.03–0.04 Å. The Shannon and Prewitt radii were derived from the oxides and fluorides, compounds that are highly ionic by comparison with the chalcogenides. If we add these ionic radii to Pauling's ionic chalcogen radii, we find that the resulting bond distances are near but deviate
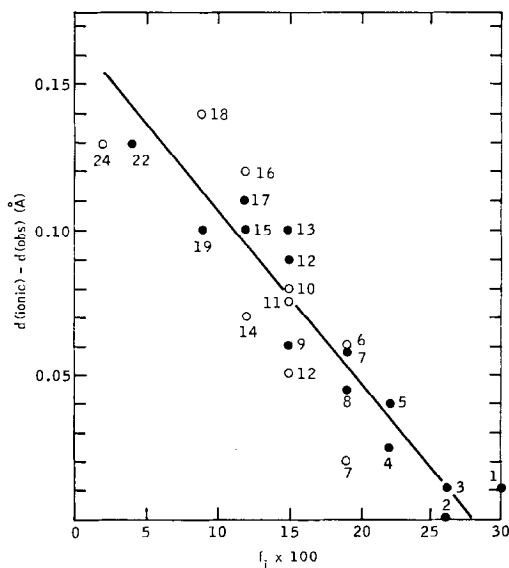


FIG. 3. The difference between the sum of the ionic radii and the observed bond lengths vs the fractional ionic character.

from those observed. In every case, the bond distance is shorter than the distance predicted from the ionic radii by an amount that increases as the ionic character decreases as shown in Fig. 3.

First, it should be pointed out that the scatter in these data is consistent with the courseness of the ionicity scale and the uncertainty in the bond lengths. Second, it should be noted that there is no correlation between the departure of the bond length from the ionic sum and the structure as has been suggested (4). Also, one must not consider the coincidence of the bond lengths in the Hf and Zr sulfides and selenides with the ionic bond lengths as evidence of complete ionic character. The sum of radii from different sets of radii (Shannon and Prewitt, Pauling) is not a reliable method for obtaining bond lengths and the bond length itself is only a very weak function of ionicity. The sum of Slater *atomic* radii give bond lengths for all these compounds of remarkable accuracy. How then are we to select an appropriate set of radii in the present context?

If we consider the atoms spherical and the chalcogens close packed, the $a$-axis parameter of the unit cell will equal the diameter of the chalcogen atom. As shown in Fig. 4, the effective chalcogen radii so defined depend on the fractional ionic character of the bond in a manner
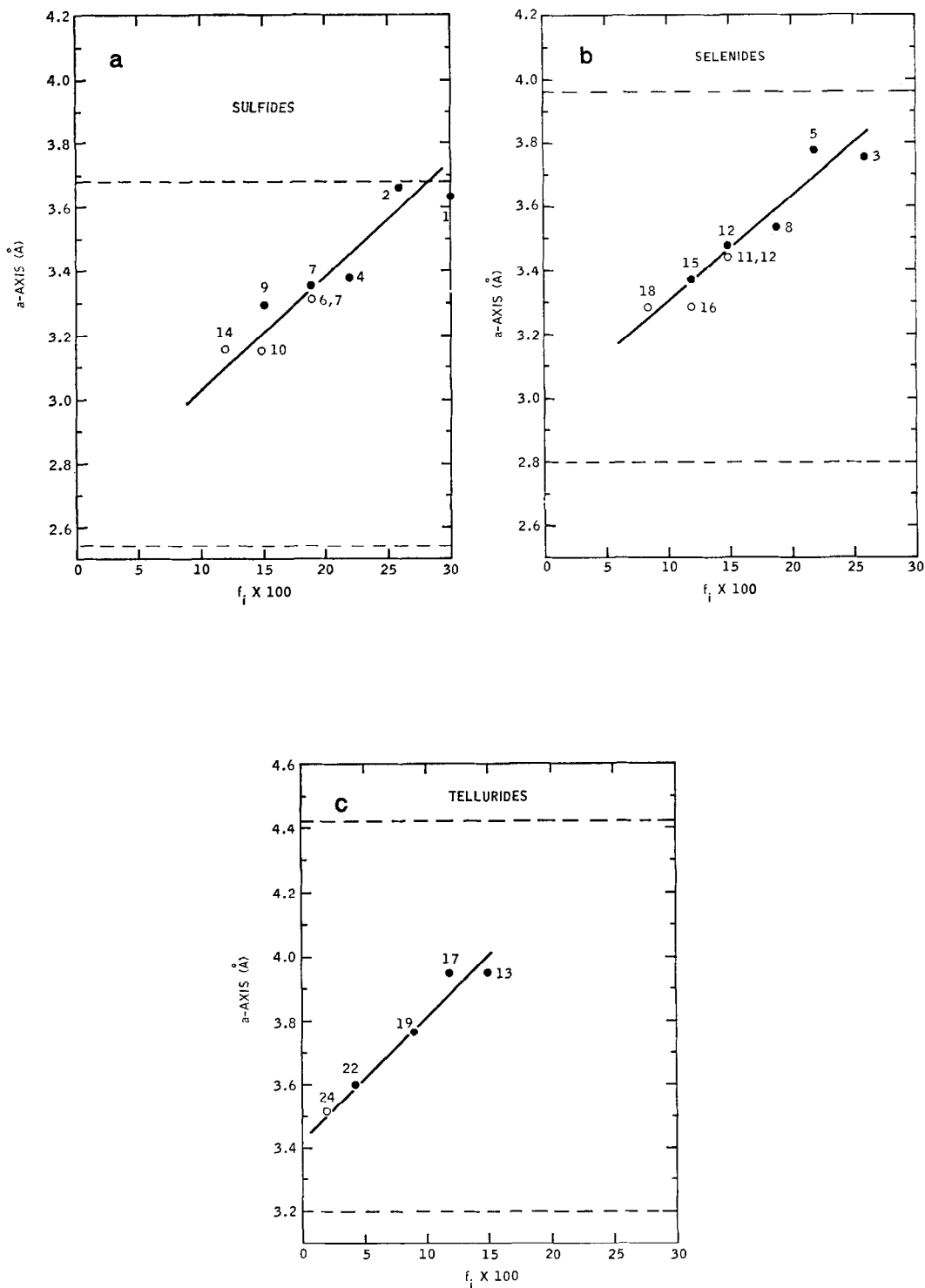
FIG. 4. The $a$-axis of the sulfides (a), selenides (b), and tellurides (c) vs $f_i$, the fractional ionic character of the metal–chalcogen bond. The upper and lower dashed lines refer respectively to the Pauling ionic and metallic diameters of the chalcogens.
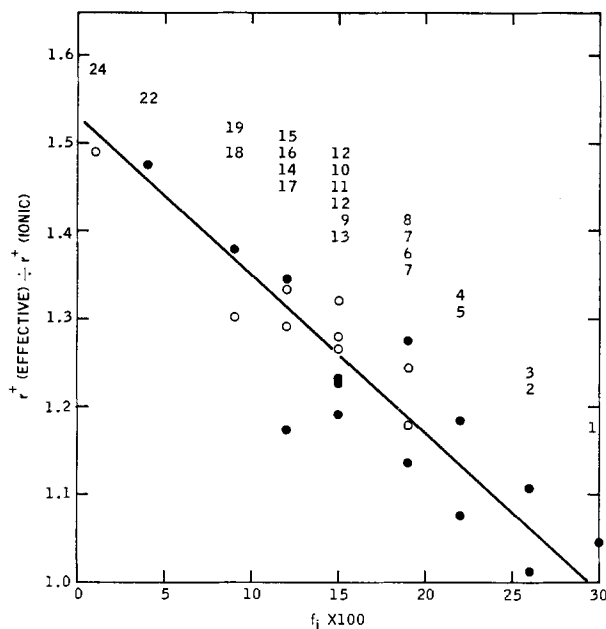
FIG. 5. The ratio of the effective cation radius to the Shannon and Prewitt ionic radius for 4+ ions in six-fold coordination vs the fractional ionic character of the metal chalcogen bond. Data for both 1T and 2H $TaS_2$ and $TaSe_2$ are presented. Error bars have been omitted for clarity. It should be noted, however, that the accuracy of the electronegativity difference $\Delta X$ cannot be better than 0.1. As this difference squared appears in the exponential expression for $f_i$, the scatter in the data would be expected to increase as $f_i$ increases. The uncertainty in bond lengths will contribute an error of $\sim \pm 0.05$ to the ratio of the radii.

in qualitative agreement with intuition. As the ionicity increases, so does the radius of the chalcogen. The chalcogen radii extrapolate to a value slightly greater than the Pauling metallic radii (7) of sulfur, selenium, and tellurium for $f_i = 0$ and to the Pauling ionic radii for $f_i \sim 0.3$. If these radii are subtracted from the observed bond distances, a set of effective metal radii are generated which are greater than the corresponding Shannon and Prewitt radii for the 4+ oxidation state by an amount that depends on $f_i$. This is shown in Fig. 5. As one might expect, the metal radii approach the Shannon and Prewitt ionic radii as $f_i$ increases.

At this point, it should be noted that a *formal* oxidation state for the metal may be extracted from the effective metal radius so defined and the dependence of ionic radius on oxidation state. The Shannon and Prewitt radii for various common oxidation states are given in Table II. From these, it can be seen that Zr and Hf compounds have radii near but greater than that of the 4+ state. Titanium in its compounds is between 2+ and 3+; vanadium between 1+ and 2+. Molybdenum and tungsten as well as

tantalum and niobium have effective radii substantially greater than any of the common oxidation states. These formal oxidation states are in remarkable accord with the effective dynamic charge found in the optical studies of Lucovsky and White (4). However, the formal nature of the oxidation states implied by the above considerations should be stressed. While it is clear the hafnium and zirconium sulfides are substantially more ionic than the molybdenum and tungsten compounds, it is unlikely that they are as ionic as the corresponding oxides and fluorides. Highly ionic compounds will not crystallize in layered structures.

### The Critical Radius Ratio

If we prepare a radius ratio-ionicity plot using these effective radii, we find that separation into two fields is once again possible, but this time a horizontal line can be drawn separating the structures. Therefore, we have prepared (Fig. 6) a plot of the compounds with $r^+$ as ordinate and $r^-$ as abscissa. The critical radius ratio is now represented by a line passing through the origin
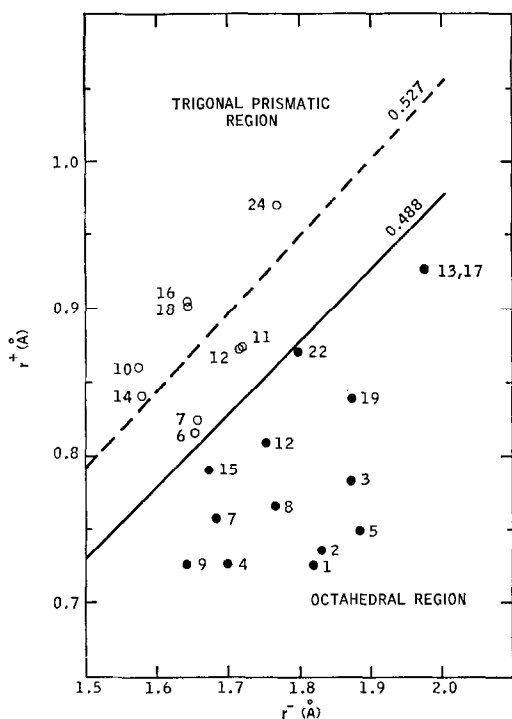
effective radii is to some extent circular in nature. However, as we have shown, the effective radii depend strongly on the elements in question and their electronegativity differences (Figs. 4 and 5). They are not arbitrarily variable. The effective radii in large measure determine which structures are permitted and not vice versa. If we view the structure question in terms of effective radii, the separation achieved in the radius ratio vs ionicity plot (Fig. 2) can be understood. The diagonal line drawn across the field will tend to become horizontal as the cations in the more covalent compounds grow at the expense of the anions.

## The Heats of Formation

There is very little thermochemical data available for the compounds under consideration, and that which is available is not very accurate because of difficulties encountered in attaining complete combustion of these compounds (16). Nonetheless, the standard heats of formation (i.e., from the elements in their standard states) reported (16, 17) are approximately proportional to the electronegativity differences squared, but with a constant of proportionality about 15% less than that proposed by Pauling. These data
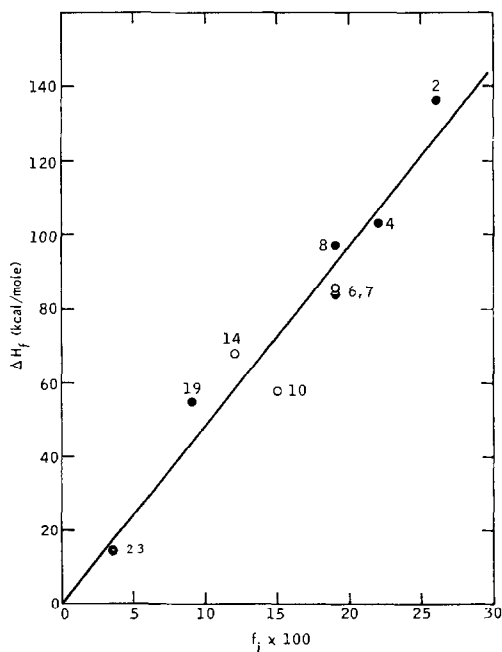
FIG. 6. A plot of the trigonal prismatic and octahedral compounds on an $r^+$ vs $r^-$ diagram. Here $r^+$ refers to the effective cation radius and $r^-$ to the a-axis divided by two. The critical radius ratio dictated by geometry and a hard sphere model, 0.527, is represented by the dashed line. The observed critical ratio is 0.49. The symbols have the same significance as in Fig. 2.

with slope equal to 0.49. The critical radius ratio at which hard spherical chalcogens on opposite sides of a layer contact is $0.527 = (7/3)^{1/2} - 1$ for trigonal prismatic coordination. It appears that the trigonal prismatic structure is maintained until the chalcogens above and below the metal atom contact and then in the case of Nb and Ta apparently deform some. (Note that the trigonal prismatic compounds that fall below the 0.527 ratio are easily converted to the octahedral phase either by quenching, slight adjustments in stoichiometry, or by the addition of small amounts of titanium.) Finally, the octahedral structure is adopted, permitting closer approach of large anions to the cation and hence the attainment of the desired bond lengths.

Because the effective radii are obtained from the stable crystal structures, the separation of the trigonal prismatic from the octahedral compounds on the basis of a critical ratio of

FIG. 7. The standard heats of formation vs the fractional ionic character. The datum for $WTe_2$ is from Ref. 18.

are shown in Fig. 7. The electronegativities used are those from Table II. When more accurate and more complete thermochemical data are gathered on these compounds, it would be interesting to see to what extent the correlations discussed in this paper might be made more exact. In particular, it should be possible to generate an electronegativity scale of greater accuracy in this *limited* context. For example, a plot of the $a$-axis of the six sulfides for which we have heats of formation vs the heat of formation shows that this parameter depends linearly on the heat of formation with much less scatter than that of Fig. 4a. The $a$-axes are known quite accurately. If we compute the rms deviation of the data from linearity in terms of the heats, we find a deviation of less than 3 kcal/mole, probably well within the experimental error in the heats of formation.

## Discussion

We have suggested that among the IVb-, Vb-, and VIb-layered dichalcogenides, where geometry permits, the compounds adopt the trigonal prismatic coordination. Trigonal prismatic coordination is not found elsewhere in the layered dichalcogenides. Those with electronic configurations $d^n$ where $n$ is 3 or greater *all* adopt the octahedral structure. If these are placed on the radius ratio ionicity plot (Fig. 2), they fall in both regions. This is not precluded by geometry. Our position is that compounds falling in the upper, trigonal-prismatic, region (i.e., compounds that are not too ionic and have a large enough radius ratio, $r^+/r^-$) have the option to adopt the trigonal prismatic structure, whereas those in the lower region do not. Compounds falling in either region can adopt the electrostatically favored octahedral structure. We must look beyond geometry to determine why those compounds ($d^n$, $n < 3$) adopting the trigonal prismatic structure do so despite the electrostatic considerations favoring octahedral coordination. Mattheiss (19) has applied the nonrelativistic, augmented-plane-wave (APW) method to calculate the electronic band structures of several of the layered transition metal dichalcogenides. By this method, he finds a hybridization gap opening in the $d$-manifold of trigonal prismatic compounds that substantially favors this structure in $MoS_2$. In as much as this gap splits off a lower two electron band from the

rest, configurations $d^n$ ($n > 2$) would probably not be so stabilized in accord with the absence of the trigonal structure in these compounds. Another consequence of this argument is that $d^0$ compounds would not have this driving force toward the trigonal prismatic structure, in accord with the octahedral structures adopted by all IVa and IVb compounds.

It is interesting to consider the consequences of altering the electronic configuration of the compound by intercalation with alkali metal atoms. If the compound $MX_2$ with a $d^n$ configuration is intercalated to form $AMX_2$ where A is an alkali metal, then the configuration is presumably $d^{n+1}$. No refined structures of these intercalation compounds are available.

Finally, we suggest that our highly local view of the bonding is consistent with the band structure calculations (19, 20) where it is found that the metal $d$ character of the conduction band and the chalcogen $p$ character of the valence band becomes less pure as one goes from the more ionic compounds to the more covalent. This trend is already clear in the diminution of the gap between valence and conduction bands as one goes from $HfS_2$ and $ZrS_2$ toward $MoTe_2$.

## References

*1.* J. A. WILSON AND A. D. YOFFE, *Advan. Phys.* **18,** 193 (1969).
*2.* T. J. WIETING AND J. L. VERBLE, *Phys. Rev. B* 3, 4286 (1971).
*3.* J. E. SMITH, M. I. NATHAN, M. W. SHAFER, AND J. B. TORRANCE, presented at 11th Int. Conf. on the Physics of Semiconductors, Warsaw (1972).
*4.* R. M. WHITE AND G. LUCOVSKY, *Solid State Commun.* **11,** 1369 (1972), See also G. LUCOVSKY AND R. M. WHITE, *Bull. Amer. Phys. Soc.* p. 452, March 1973, and G. LUCOVSKY, R. M. WHITE, J. A. BENDA, AND J. F. REVELLI, *Phys. Rev. B* **7,** 3859 (1973).
*5.* J. C. MCMENAMIN AND W. E. SPICER, *Phys. Rev. Lett.* **29,** 1501 (1972).
*6.* R. HUISMAN, R. DEJONGE, C. HAAS, AND F. JELLINEK, *J. Solid State Chem.* **3,** 56 (1971).

7. L. PAULING, "The Nature of the Chemical Bond," 3rd ed., Cornell University Press, Ithaca (1960).

8. J. C. PHILLIPS, *J. Appl. Phys.* **43**, 3560 (1972).

9. R. D. SHANNON AND C. T. PREWITT, *Acta Crystallog.* **B25**, 925 (1969).

10. J. C. SLATER, *J. Chem. Phys.* **41**, 3199 (1964).

11. F. JELLINEK, *Ark. Kemi* **20**, 447 (1962).

12. A. H. THOMPSON, F. R. GAMBLE, AND J. F. REVELLI, *Solid State Commun.* **9**, 981 (1971).

13. B. E. BROWN AND D. J. BEERNTSEN, *Acta Crystallog.* **18**, 31 (1965).

14. M. MAREZIO, P. D. DERNIER, A. MENTH, AND G. W. HULL, JR., *J. Solid State Chem.* **4**, 425 (1972).

15. J. G. SMEGGIL AND S. BARTRAM, *J. Solid State Chem.* **5**, 391 (1973).

16. J. BEAR AND F. K. MCTAGGART, *Australian J. Chem.* **11**, 458 (1958).

17. J. G. GIBSON AND J. L. SUDWORTH, "Specific Energies of Galvanic Reactions and Related Thermodynamic Date," p. 159, Chapman and Hall Ltd., London (1973).

18. A. A. OPALOVSKII, V. E. FEDOROV, E. V. LOBKOV, AND B. I. TSIKANOVSKII, *Zh. Fiz. Khim.* **45**, 1864 (1971).

19. L. F. MATTHEISS, *Phys. Rev. Lett.* **30**, 724 (1973).

20. R. V. KASOWSKI, *Phys. Rev. Lett.* **30**, 1175 (1973).